

Non-Abelian Statistics in one dimension: topological momentum spacings and SU(2) level k fusion rules

Martin Greiter,¹ F.D.M. Haldane,² and Ronny Thomale¹

¹*Institute for Theoretical Physics, University of Würzburg, Am Hubland, D-97074 Würzburg, Germany*

²*Department of Physics, Princeton University, Princeton, New Jersey 08544, USA*

(Dated: May 24, 2019)

We use a family of critical spin chain models discovered recently by one of us [M. Greiter, *Mapping of Parent Hamiltonians*, Springer, Berlin/Heidelberg 2011] to propose and elaborate that non-Abelian, SU(2) level $k = 2S$ anyon statistics manifests itself in one dimension through topological selection rules for fractional shifts in the spacings of linear momenta, which yield an internal Hilbert space of, in the thermodynamic limit degenerate states. These shifts constitute the equivalent to the fractional shifts in the relative angular momenta of anyons in two dimensions. We derive the rules first for Ising anyons, and then generalize them to SU(2) level k anyons. We establish a one-to-one correspondence between the topological choices for the momentum spacings and the fusion rules of spin $\frac{1}{2}$ spinons in the SU(2) level k Wess–Zumino–Witten model, where the internal Hilbert space is spanned by the manifold of allowed fusion trees in the Bratelli diagrams. Finally, we show that the choices in the fusion trees may be interpreted as the choices between different domain walls between the $2S + 1$ possible, degenerate dimer configurations of the spin S chains at the multicritical point.

I. INTRODUCTION

The concept of fractional quantization, and, in particular, fractional statistics¹, is witnessing a renaissance of interest in recent years. This is due to possible applications of states supporting excitations with non-Abelian statistics² to the rapidly evolving field of quantum computing and cryptography. The paradigm for this class is the Pfaffian state^{3,4}, which has been proposed to describe the experimentally observed quantized Hall plateau at Landau level filling fraction $\nu = \frac{5}{2}$ ⁴. The state supports quasiparticle excitations which possess Majorana fermion states at zero energy⁵. Braiding of these half-vortices yields non-trivial changes in the occupations of the Majorana fermion states, and hence renders the exchanges non-commutative or non-Abelian^{6,7}. Since this “internal” state vector is insensitive to local perturbations, it is preeminently suited for applications as protected qubits in quantum computation^{8,9}. Non-Abelian anyons are further established in other quantum Hall states including Read-Rezayi states¹⁰, in the non-Abelian phase of the Kitaev model¹¹, the Yao–Kivelson and Yao–Lee models^{12,13}, and in the family of non-Abelian chiral spin liquid (NACSL) states introduced by two of us^{14–16}. The latter were subsequently revisited from a coupled ladder approach^{17,18}, continuum limit interpolation¹⁹, as well as from the viewpoint of Gutzwiller-projected superconductors²⁰ and topological entanglement entropy²¹.

In this article, we propose and elaborate that the possibility of non-Abelian statistics is not limited to two spatial dimensions, but exists in certain families of one dimensional spin models as well. In particular, we use a family of (multi-) critical spin chain models discovered recently by one of us²² (and for SU(2) level 2 shortly thereafter independently obtained by Nielsen et al.²³), to show that the SU(2) level k anyon statistics of the spinons of these models manifests itself in one dimen-

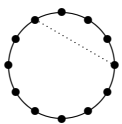
sion through topological selection rules for the fractional momentum spacings, which constitute the equivalent to fractional relative angular momentum for anyons in two dimensions. In Section II, we review the fractional momentum spacings of the spinons excitation in an $1/r^2$ model discovered by Shastry and one of us, commonly referred to as the Haldane–Shastry model^{24,25}. This model constitutes a lattice Wess–Zumino–Witten model^{26–28}, and the spinons obey Abelian half-Fermi statistics^{29,30}. We further review the formalism of extended Young tableaux^{31,32}, which provides the single particle momenta of the spinon excitations. In Section III, we first review the ground state and the associated parent Hamiltonian of a similar, exactly solvable, critical spin model for a spin $S = 1$ chain^{22,23,33}. This model supports spinon excitations with Ising-type, non-Abelian statistics. We then generalize the formalism of extended Young tableaux³¹ to the case $S = 1$ and find that after every second spinon, there are two possible choices for the quantization of the momentum spacing—it can either be integer or half integer. This yields an equivalent number of choices as we would obtain if we had one Majorana fermion state for each spinon, in analogy to the Majorana fermion states located at the quasiparticles of the Moore–Read state in the quantum Hall effect^{3,5,34}. The choice we have after the 1st, 3rd, 5th etc. spinon is that the spacings between the neighboring single spinon momenta can either be that of Bose (or Fermi) statistics, or be that of half-Fermi statistics. We call the momentum spacings for this model Majorana spacings. In Section IV, we review the generalization of the model to arbitrary spin S , generalize the formalism of extended Young tableaux accordingly, and derive the rules for the momentum spacings of non-Abelian SU(2) level $k = 2S$ anyons. These are not as easily stated, but reasonably simple as far as the principles are concerned. The mapping of these rules back to the related family of quantized Hall states, the Read-Rezayi states¹⁰, may be instructive in formulating explicit ma-

trix representations of $SU(2)$ level k anyons in two dimensions, a task which so far has been accomplished only for Ising anyons⁶. Finally, we establish a one-to-one correspondence between the rules for the momentum spacings we have derived from the formalism of extended Young tableaux, and the fusion rules of $j = \frac{1}{2}$ spinons within the $SU(2)$ level $k = 2S$ algebra. The physical information regarding the momentum spacings can hence be transferred to the spinon bases^{35–38} of the conformal field theory, the Wess–Zumino–Witten model^{26,27,39,40}.

II. FRACTIONAL MOMENTUM SPACINGS AND ABELIAN ANYONS IN 1D

A. The Haldane–Shastry model

The Haldane–Shastry model^{24,25,31,41–47} is one of the most important paradigms for a generic spin $\frac{1}{2}$ liquid on a chain. Consider a spin $\frac{1}{2}$ chain with periodic boundary conditions and an even number of sites N on a unit circle embedded in the complex plane:



N sites with spin $\frac{1}{2}$ on unit circle:
 $\eta_\alpha = e^{i\frac{2\pi}{N}\alpha}$ with $\alpha = 1, \dots, N$

The $1/r^2$ -Hamiltonian

$$H^{\text{HS}} = \left(\frac{2\pi}{N}\right)^2 \sum_{\alpha < \beta} \frac{\mathbf{S}_\alpha \mathbf{S}_\beta}{|\eta_\alpha - \eta_\beta|^2}, \quad (1)$$

where $|\eta_\alpha - \eta_\beta|$ is the chord distance between the sites α and β , has the exact ground state

$$|\psi_0^{\text{HS}}\rangle = \sum_{\{z_1, \dots, z_M\}} \psi_0^{\text{HS}}(z_1, \dots, z_M) S_{z_1}^+ \cdots S_{z_M}^+ |\underbrace{\downarrow \downarrow \dots \downarrow}_{\text{all } N \text{ spins } \downarrow}\rangle, \quad (2)$$

where the sum extends over all possible ways to distribute the $M = \frac{N}{2}$ \uparrow -spin coordinates z_i on the unit circle and

$$\psi_0^{\text{HS}}(z_1, z_2, \dots, z_M) = \prod_{i < j} (z_i - z_j)^2 \prod_{i=1}^M z_i. \quad (3)$$

The ground state is real, a spin singlet, has momentum

$$p_0 = -\frac{\pi}{2}N, \quad (4)$$

where we have adopted a convention according to which the “vacuum” state $|\downarrow \downarrow \dots \downarrow\rangle$ has momentum $p = 0$ (and the empty state $|0\rangle$ has $p = \pi(N - 1)$), and energy

$$E_0 = -\frac{\pi^2}{24} \left(N + \frac{5}{N}\right). \quad (5)$$

The ground state (2) with (3) was known long before the model, as it can be obtained by Gutzwiller projection from Slater determinant states describing filled bands^{48–50}. The Hamiltonian (1) possesses a Yangian symmetry^{43,51}, is fully integrable⁵², and also amenable to exact solution via the asymptotic Bethe Ansatz^{41,44,51,53}.

We will not verify the model explicitly here, but rather focus on the fractional momentum spacings of the spinon excitations, which reflect their Abelian anyon statistics.

B. Spinon excitations and fractional statistics

The elementary excitations for the Haldane–Shastry model are free spinon excitations, which carry spin $\frac{1}{2}$ and no charge. They constitute an instance of fractional quantization, which is both conceptually and mathematically similar to the fractional quantization of charge in the fractional quantum Hall effect⁵⁴. Their fractional quantum number is the spin, which takes the value $\frac{1}{2}$ in a Hilbert space (2) made out of spin flips S^+ , which carry spin 1.

One-spinon states.—To write the wave function for a \downarrow -spin spinon localized at site η_α , consider a chain with an odd number of sites N and let $M = \frac{N-1}{2}$ be the number of \uparrow or \downarrow spins condensed in the uniform liquid. The spinon wave function is then given by

$$\psi_{\alpha\downarrow}(z_1, z_2, \dots, z_M) = \prod_{i=1}^M (\eta_\alpha - z_i) \psi_0^{\text{HS}}(z_1, z_2, \dots, z_M), \quad (6)$$

which we understand substituted into (2). It is easy to verify $S_{\text{tot}}^z \psi_{\alpha\downarrow} = -\frac{1}{2} \psi_{\alpha\downarrow}$ and $S_{\text{tot}}^- \psi_{\alpha\downarrow} = 0$, which shows that the spinon transforms as a spinor under rotations.

The localized spinon (6) is not an eigenstate of the Hamiltonian (1). To obtain exact eigenstates, we construct momentum eigenstates according to

$$\psi_{m\downarrow}(z_1, z_2, \dots, z_M) = \sum_{\alpha=1}^N (\bar{\eta}_\alpha)^m \psi_{\alpha\downarrow}(z_1, z_2, \dots, z_M), \quad (7)$$

where the integer m corresponds to a momentum quantum number. Since $\psi_{\alpha\downarrow}(z_1, z_2, \dots, z_M)$ contains only powers $\eta_\alpha^0, \eta_\alpha^1, \dots, \eta_\alpha^M$ and

$$\sum_{\alpha=1}^N \bar{\eta}_\alpha^m \eta_\alpha^n = \delta_{mn} \pmod{N}, \quad (8)$$

$\psi_{m\downarrow}(z_1, z_2, \dots, z_M)$ will vanish unless $m = 0, 1, \dots, M$. There are only roughly half as many-spinon orbitals as there are sites. Spinons on neighboring sites hence cannot be orthogonal. Acting with (1) on (7), we obtain^{22,41,46,55}

$$H^{\text{HS}} |\psi_{m\downarrow}\rangle = \left[-\frac{\pi^2}{24} \left(N - \frac{1}{N}\right) + \frac{2\pi^2}{N^2} m(M - m) \right] |\psi_{m\downarrow}\rangle. \quad (9)$$

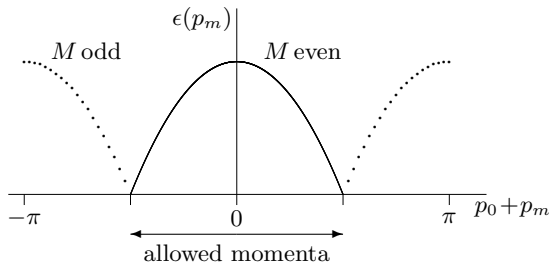


FIG. 1. Dispersion of a single spinon in a Haldane–Shastry chain.

To make a correspondence between m and the spinon momentum p_m , we translate (7) counterclockwise by one lattice spacing (which we set to unity for present purposes) around the unit circle,

$$\mathbf{T} |\psi_{m\downarrow}\rangle = e^{i(p_0+p_m)} |\psi_{m\downarrow}\rangle. \quad (10)$$

With $p_0 = -\frac{\pi}{2}N$, we find

$$p_m = \pi - \frac{2\pi}{N} \left(m + \frac{1}{4} \right). \quad (11)$$

The energy (9) can be written as $E = E_0 + \epsilon(p_m)$, with the spinon dispersion given by

$$\epsilon(p) = \frac{1}{2}p(\pi - p) + \frac{\pi^2}{8N^2}, \quad (12)$$

as depicted in Figure 1. The interval of allowed spinon momenta spans only half of the Brillouin zone, and alternates with M even vs. M odd.

Two-spinon states.—To write the wave function for two \downarrow -spin spinons localized at sites η_α and η_β , consider a chain with N even and $M = \frac{N-2}{2}$. The two-spinon state is then given by

$$\psi_{\alpha\beta}(z_1, \dots, z_M) = \prod_{i=1}^M (\eta_\alpha - z_i)(\eta_\beta - z_i) \psi_0^{\text{HS}}(z_1, \dots, z_M). \quad (13)$$

A momentum basis for the two-spinon states is given by

$$\psi_{mn}(z_1, \dots, z_M) = \sum_{\alpha, \beta=1}^N (\bar{\eta}_\alpha)^m (\bar{\eta}_\beta)^n \psi_{\alpha\beta}(z_1, \dots, z_M), \quad (14)$$

where $M \geq m \geq n \geq 0$. For m or n outside this range, ψ_{mn} vanishes identically, reflecting the overcompleteness of the position space basis. Acting with (1) on (7), we obtain^{22,41,46,55}

$$H^{\text{HS}} |\psi_{mn}\rangle = E_{mn} |\psi_{mn}\rangle + \sum_{l=1}^{l_{\max}} V_l^{mn} |\psi_{m+l, n-l}\rangle \quad (15)$$

with

$$E_{mn} = -\frac{\pi^2}{24} \left(N - \frac{19}{N} + \frac{24}{N^2} \right) + \frac{2\pi^2}{N^2} \left[m \left(\frac{N}{2} - 1 - m \right) + n \left(\frac{N}{2} - 1 - n \right) - \frac{m-n}{2} \right], \quad (16)$$

$$V_l^{mn} = -\frac{2\pi^2}{N^2} (m - n + 2l), \quad (17)$$

and $l_{\max} = \min(M - m, n)$. Since the “scattering” of the non-orthogonal basis states $|\psi_{mn}\rangle$ in (15) only occurs in one direction, increasing $m - n$ while keeping $m + n$ fixed, the eigenstates of H^{HS} have energy eigenvalues E_{mn} , and are of the form

$$|\phi_{mn}\rangle = \sum_{l=0}^{l_M} a_l^{mn} |\psi_{m+l, n-l}\rangle. \quad (18)$$

A recursion relation for the coefficients a_l^{mn} is readily obtained from (15).

If we identify the single-spinon momenta for $m \geq n$ according to

$$p_m = \pi - \frac{2\pi}{N} \left(m + \frac{1}{2} + s \right), \quad (19)$$

$$p_n = \pi - \frac{2\pi}{N} \left(n + \frac{1}{2} - s \right), \quad (20)$$

with a statistical shift $s = \frac{1}{4}$ ^{47,56}, we can write the energy

$$E_{mn} = E_0 + \epsilon(p_m) + \epsilon(p_n), \quad (21)$$

where E_0 is the ground state energy (5) and $\epsilon(p)$ the spinon dispersion (12).

Fractional statistics.—The mutual half-Fermi statistics of the spinons manifests itself in the fractional shift s in the single-spinon momenta (19) and (20), as we will elaborate now³⁰. The Ansatz (14) unambiguously implies that the sum of the two spinon momenta is given by $q_m + q_n = 2\pi - \frac{2\pi}{N}(m + n + 1)$, and hence (19) and (20). The shift s is determined by demanding that the excitation energy (21) of the two-spinon state is a sum of single-spinon energies, which in turn is required for the explicit solution here to be consistent with the models solution via the asymptotic Bethe ansatz^{51,56,57}.

The shift decreases the momentum p_m of spinon 1 and increases momentum p_n of spinon 2. This may surprise at first as the basis states (14) are constructed symmetrically with regard to interchanges of m and n . To understand the asymmetry, note that $M \geq m \geq n \geq 0$ implies $0 < p_m < p_n < \pi$. The dispersion (12) implies that the group velocity of the spinons is given by

$$v_g(p) = \partial_p \epsilon(p) = \frac{\pi}{2} - p, \quad (22)$$

which in turn implies that $v_g(p_m) > v_g(p_n)$. This means that the *relative motion* of spinon 1 (with q_m) with respect to spinon 2 (with q_n) is *always counterclockwise* on

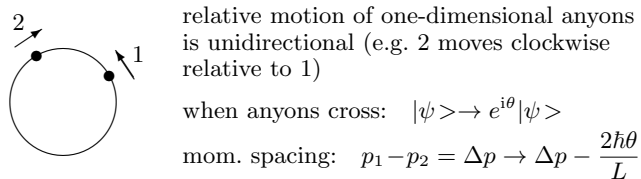


FIG. 2. Fractional statistics in one dimension. The crossings of the anyons are unidirectional, and the many particle wave function acquires a statistical phase θ whenever they cross.

the unit circle (see Figure 2). The shifts in the individual spinon momenta can hence be explained by assuming that the two-spinon state acquires a statistical phase $\theta = 2\pi s$ whenever the spinons pass through each other. This phase implies that q_m is shifted by $-\frac{2\pi}{N}s$ since we have to translate spinon 1 counterclockwise through spinon 2 and hence counterclockwise around the unit circle when obtaining the allowed values for q_m from the PBCs. Similarly, q_n is shifted by $+\frac{2\pi}{N}s$ since we have to translate spinon 2 clockwise through spinon 1 and hence clockwise around the unit circle when obtaining the quantization of q_n .

That the crossing of the spinons occurs only in one direction is a necessary requirement for fractional statistics to exist in one dimension. If the spinons could cross in both directions, the fact that paths interchanging them twice (i.e., once in each direction) are topologically equivalent to paths not interchanging them at all would imply $2\theta = 0 \pmod{2\pi}$ for the statistical phase, i.e., only allow for the familiar choices of bosons or fermions. With the scattering occurring in only one direction, arbitrary values for θ are possible. Note that the one-dimensional anyons break neither time-reversal symmetry (T) nor parity (P).

The fractional statistics of the spinons manifests itself further in the fractional exclusion (or generalized Pauli) principle introduced by one of us²⁹. If we consider a state with L spinons, we can easily see from (7), (8), and (14) that the number of orbitals available for further spinons we may wish to create is $M + 1$, where $M = \frac{N-L}{2}$ is the number of \uparrow or \downarrow spins in the remaining uniform liquid. (In this representation, the spinon wave functions are symmetric; two or more spinons can have the same value for m .) In other words, the creation of *two* spinons reduces the number of available single spinon states by *one*. They hence obey half-Fermi statistics in the sense of the generalized Pauli exclusion principle. (For fermions, the creation of two particles would decrease the number of available single particle by two, while this number would not change for bosons.)

C. Young tableaux and many-spinon states

The easiest way to obtain the spectrum of the model is through the one-to-one correspondence between the

$$\begin{array}{l}
 \underbrace{\begin{array}{|c|} \hline 1 \\ \hline \end{array}} \otimes \underbrace{\begin{array}{|c|} \hline 2 \\ \hline \end{array}} \otimes \underbrace{\begin{array}{|c|} \hline 3 \\ \hline \end{array}} = \begin{array}{|c|} \hline 1 \\ \hline 2 \\ \hline 3 \\ \hline \end{array} \oplus \begin{array}{|c|c|} \hline 1 & 2 \\ \hline 3 \\ \hline \end{array} \oplus \begin{array}{|c|c|} \hline 1 & 3 \\ \hline 2 \\ \hline \end{array} \oplus \begin{array}{|c|c|c|} \hline 1 & 2 & 3 \\ \hline \end{array} \\
 S=0 & S=1 & S=\frac{1}{2} & S=\frac{1}{2} & S=\frac{3}{2}
 \end{array}$$

FIG. 3. Total spin representations of three $S = \frac{1}{2}$ spins with Young tableaux. For $SU(n)$ with $n > 2$, the tableaux with three boxes on top of each other would exist as well.

Young tableaux classifying the total spin representations of N spins and the exact eigenstates of the the Haldane–Shastry model for a chain with N sites, which are classified by the total spins and the fractionally spaced single-particle momenta of the spinons³¹.

This correspondence yields the allowed sequences of single-spinon momenta p_1, \dots, p_L as well as the allowed representations for the total spin of the states such that the eigenstates of the Haldane–Shastry model have momenta and energies

$$p = p_0 + \sum_{i=1}^L p_i, \quad E = E_0 + \sum_{i=1}^L \epsilon(p_i), \quad (23)$$

where p_0 and E_0 denote the ground state momentum and energy, respectively, and $\epsilon(p)$ is the single-spinon dispersion. The correspondence hence does not only provide the quantum numbers of all the states in the spectrum, but also shows that it is sensible to view the individual spinons as particles, rather than just as solitons or collective excitations in many body condensates. We now proceed by stating these rules without further motivating or even deriving them.

To begin with, the Hilbert space of a system of N identical $SU(n)$ spins can be decomposed into representations of the total spin, which commutes with (1) and hence can be used to classify the eigenstates. These representations are compatible with the representations of the symmetric group S_N of N elements, which may be expressed in terms of Young tableaux^{58,59}. The general rule for obtaining Young tableaux is illustrated for three $S = \frac{1}{2}$ spins in Fig. 3. For each of the N spins, draw a box and number the boxes consecutively from left to right. The representations of $SU(n)$ are constructed by putting the boxes together such that the numbers assigned to them increase in each row from left to right and in each column from top to bottom. Each tableau indicates symmetrization over all boxes in the same row, and antisymmetrization over all boxes in the same column. This implies that we cannot have more than n boxes on top of each other for $SU(n)$ spins. For $SU(2)$, each tableau corresponds to a spin $S = \frac{1}{2}(\lambda_1 - \lambda_2)$ representation, with λ_i the number of boxes in the i th row, and stands for a multiplet $S^z = -S, \dots, S$.

The one-to-one correspondence between the Young tableaux and the non-interacting many-spinon eigen-

	S_{tot}			L	a_1, \dots, a_L	p_{tot}		
$\begin{array}{ c c } \hline 1 & 3 \\ \hline 2 & 4 \\ \hline \end{array}$	0	\rightarrow	$\begin{array}{ c c } \hline 1 & 3 \\ \hline 2 & 4 \\ \hline \end{array}$	\rightarrow	$\begin{array}{ c c } \hline 1 & 3 \\ \hline 2 & 4 \\ \hline \end{array}$	0	-----	0
$\begin{array}{ c c } \hline 1 & 2 \\ \hline 3 & 4 \\ \hline \end{array}$	0	\rightarrow	$\begin{array}{ c c } \hline 1 & 2 \\ \hline 3 & 4 \\ \hline \end{array}$	\rightarrow	$\begin{array}{ c c } \hline 1 & 2 \\ \hline \bullet & 3 \\ \hline \bullet & 4 \\ \hline \end{array}$	2	$\bullet \text{---} \bullet$ 1 4	π
$\begin{array}{ c c c } \hline 1 & 3 & 4 \\ \hline 2 & & \\ \hline \end{array}$	1	\rightarrow	$\begin{array}{ c c c } \hline 1 & 3 & 4 \\ \hline 2 & & \\ \hline \end{array}$	\rightarrow	$\begin{array}{ c c c } \hline 1 & 3 & 4 \\ \hline 2 & \bullet & \bullet \\ \hline \end{array}$	2	$\text{---} \bullet \text{---} \bullet$ 3 4	$\frac{3\pi}{2}$
$\begin{array}{ c c c } \hline 1 & 2 & 4 \\ \hline 3 & & \\ \hline \end{array}$	1	\rightarrow	$\begin{array}{ c c c } \hline 1 & 2 & 4 \\ \hline 3 & & \\ \hline \end{array}$	\rightarrow	$\begin{array}{ c c c } \hline 1 & 2 & 4 \\ \hline \bullet & 3 & \bullet \\ \hline \end{array}$	2	$\bullet \text{---} \bullet$ 1 4	π
$\begin{array}{ c c c } \hline 1 & 2 & 3 \\ \hline 4 & & \\ \hline \end{array}$	1	\rightarrow	$\begin{array}{ c c c } \hline 1 & 2 & 3 \\ \hline 4 & & \\ \hline \end{array}$	\rightarrow	$\begin{array}{ c c c } \hline 1 & 2 & 3 \\ \hline \bullet & \bullet & 4 \\ \hline \end{array}$	2	$\bullet \text{---} \bullet \text{---}$ 1 2	$\frac{\pi}{2}$
$\begin{array}{ c c c c } \hline 1 & 2 & 3 & 4 \\ \hline \end{array}$	2	\rightarrow	$\begin{array}{ c c c c } \hline 1 & 2 & 3 & 4 \\ \hline \end{array}$	\rightarrow	$\begin{array}{ c c c c } \hline 1 & 2 & 3 & 4 \\ \hline \bullet & \bullet & \bullet & \bullet \\ \hline \end{array}$	4	$\bullet \text{---} \bullet \text{---} \bullet \text{---} \bullet$ 1 2 3 4	0

FIG. 4. Young tableau decomposition and the corresponding spinon states for an $S = \frac{1}{2}$ spin chain with $N = 4$ sites. The dots represent the spinons. The spinon momentum numbers a_i are given by the numbers in the boxes of the same column. Note that $\sum(2S_{\text{tot}} + 1) = 2^N$.

states of the Haldane–Shastry model is illustrated in Fig. 4 for a chain with $N = 4$ sites. The rule is that in each Young tableau, we shift boxes to the right such that each box is below or in the column to the right of the box with the preceding number. Each missing box in the resulting, extended tableaux represents a spinon. The extended tableaux provide us with the total spin of each multiplet, which is given by the representation specified by the original Young tableau, the number L of spinons present, and the individual spinon momentum numbers a_i , which are just the numbers in the boxes above or below the dots representing the spinons. The single-spinon momenta are obtained from those via

$$p_i = \frac{\pi}{N} \left(a_i - \frac{1}{2} \right), \quad (24)$$

which implies $\delta \leq p_i \leq \pi - \delta$, with $\delta = \frac{\pi}{2N} \rightarrow 0$ for $N \rightarrow \infty$.

The total momentum and the total energies of the many-spinon states are given by (23) with

$$p_0 = -\frac{\pi}{2} N, \quad E_0 = -\frac{\pi^2}{24} \left(N + \frac{5}{N} \right), \quad (25)$$

and the single-spinon dispersion

$$\epsilon(p) = \frac{1}{2} p(\pi - p) + \frac{\pi^2}{8N^2}, \quad (26)$$

where we use a convention according to which the “vacuum” state $|\downarrow\downarrow \dots \downarrow\rangle$ has momentum $p = 0$ (and the empty state $|0\rangle$ has $p = \pi(N - 1)$).

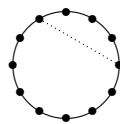
This correspondence shows that spinons are non-interacting, with momentum spacings appropriate for half-fermions. We may interpret the Haldane–Shastry

model as a reparameterization of a Hilbert space spanned by spin flips (2) into a basis which consists of the Haldane–Shastry ground state plus all possible many-spinon states.

III. MAJORANA SPACINGS AND ISING ANYONS

A. An exact model of a critical $S = 1$ spin chain described by a Pfaffian

As for the Haldane–Shastry model, we consider a one-dimensional lattice with periodic boundary conditions and an even number of sites N on a unit circle embedded in the complex plane. The only difference is that now the spin on each site is $S = 1$:



N sites with spin 1 on unit circle:

$$\eta_\alpha = e^{i\frac{2\pi}{N}\alpha} \quad \text{with } \alpha = 1, \dots, N$$

The ground state wave function we consider here^{14,22,60} is given by a bosonic Pfaffian state in the complex lattice coordinates z_i supplemented by a phase factor,

$$\psi_0^{S=1}(z_1, z_2, \dots, z_N) = \text{Pf} \left(\frac{1}{z_i - z_j} \right) \prod_{i < j}^N (z_i - z_j) \prod_{i=1}^N z_i. \quad (27)$$

The Pfaffian is given by the fully antisymmetrized sum over all possible pairings of the N particle coordinates,

$$\text{Pf} \left(\frac{1}{z_i - z_j} \right) \equiv \mathcal{A} \left\{ \frac{1}{z_1 - z_2} \cdot \dots \cdot \frac{1}{z_{N-1} - z_N} \right\}. \quad (28)$$

The “particles” z_i represent re-normalized spin flips \tilde{S}_α^+ acting on a vacuum with all spins in the $S^z = -1$ state,

$$|\psi_0^{S=1}\rangle = \sum_{\{z_1, \dots, z_N\}} \psi_0^{S=1}(z_1, \dots, z_N) \tilde{S}_{z_1}^+ \cdots \tilde{S}_{z_N}^+ |-1\rangle_N, \quad (29)$$

where the sum extends over all possibilities of distributing the N “particles” over the N lattice sites allowing for double occupation,

$$\tilde{S}_\alpha^+ \equiv \frac{S_\alpha^z + 1}{2} S_\alpha^+, \quad (30)$$

and

$$|-1\rangle_N \equiv \otimes_{\alpha=1}^N |1, -1\rangle_\alpha. \quad (31)$$

This state is translationally invariant with momentum $p_0 = 0$, a spin singlet, real, and invariant under P and T. It may be viewed as the one-dimensional analog of the non-Abelian chiral spin liquid^{14,16}.

Like the ground state of the Haldane–Shastry model, the $S = 1$ state (27) describes a critical spin liquid in one dimension, with algebraically decaying correlations. It does not, however, serve as a paradigm of the generic $S = 1$ spin state, as the generic state possesses a Haldane gap^{61–64} in the spin excitation spectrum due to linearly confining forces between the spinons^{60,65–68}.

The $S = 1$ Pfaffian state (29) with (27) is the exact ground state of the Hamiltonian^{22,33}

$$H^{S=1} = \frac{2\pi^2}{N^2} \left[\sum_{\alpha \neq \beta}^N \frac{\mathbf{S}_\alpha \mathbf{S}_\beta}{|\eta_\alpha - \eta_\beta|^2} - \frac{1}{20} \sum_{\substack{\alpha, \beta, \gamma \\ \alpha \neq \beta, \gamma}}^N \frac{(\mathbf{S}_\alpha \mathbf{S}_\beta)(\mathbf{S}_\alpha \mathbf{S}_\gamma) + (\mathbf{S}_\alpha \mathbf{S}_\gamma)(\mathbf{S}_\alpha \mathbf{S}_\beta)}{(\tilde{\eta}_\alpha - \tilde{\eta}_\beta)(\eta_\alpha - \eta_\gamma)} \right], \quad (32)$$

with energy eigenvalue

$$E_0^{S=1} = -\frac{2\pi^2}{15} \left(N + \frac{5}{N} \right). \quad (33)$$

This model was shortly afterwards independently rediscovered by Nielsen, Cirac, and Sierra²³. The effective field theory of the Hamiltonian (32) is given by the SU(2) level $k = 2$ Wess–Zumino–Witten model^{26,27,39,40}. It was further shown very recently by Michaud et al.⁶⁹ that one can construct a critical spin model of the Wess–Zumino–Witten universality class if one only keeps the leading two- and three-body spin terms in (32), and adjusts the coefficients accordingly.

In analogy to the non-Abelian quasiparticles of the Pfaffian state in the quantized Hall effect, the spinons of the model are Ising anyons. The space of the (in the thermodynamic limit) degenerate states associated with the non-Abelian statistics is spanned by the Majorana fermion orbitals at the quasiparticle or spinon excitations. The model hence provides us with a framework to study Ising anyons in one dimension.

B. Generation of the ground state by projection from Gutzwiller states

We will show now that the $S = 1$ ground state (27) can alternatively be generated by considering two (identical) Haldane–Shastry or Gutzwiller states (3) and projecting onto the triplet or $S = 1$ configuration contained in

$$\frac{1}{2} \otimes \frac{1}{2} = \mathbf{0} \oplus \mathbf{1} \quad (34)$$

at each site^{14,60}.

This projection can be accomplished very conveniently using Schwinger bosons^{70,71}. In terms of those, the SU(2) spin operators are given by

$$\mathbf{S} = \frac{1}{2} (a^\dagger, b^\dagger) \boldsymbol{\sigma} \begin{pmatrix} a \\ b \end{pmatrix}, \quad (35)$$

where $\boldsymbol{\sigma} = (\sigma_x, \sigma_y, \sigma_z)$ is the vector consisting of the three Pauli matrices, and a^\dagger, b^\dagger (a, b) are independent boson creation (annihilation) operators which obey

$$\begin{aligned} [a, a^\dagger] &= [b, b^\dagger] = 1, \\ [a, b] &= [a, b^\dagger] = [a^\dagger, b] = [a^\dagger, b^\dagger] = 0. \end{aligned} \quad (36)$$

The spin quantum number S is given by half the number of bosons,

$$2S = a^\dagger a + b^\dagger b, \quad (37)$$

and the usual spin states (simultaneous eigenstates of \mathbf{S}^2 and S^z) are given by

$$|S, m\rangle = \frac{(a^\dagger)^{S+m} (b^\dagger)^{S-m}}{\sqrt{(S+m)!} \sqrt{(S-m)!}} |0\rangle. \quad (38)$$

In particular, the spin- $\frac{1}{2}$ states are given by

$$|\uparrow\rangle = c_\uparrow^\dagger |0\rangle = a^\dagger |0\rangle, \quad |\downarrow\rangle = c_\downarrow^\dagger |0\rangle = b^\dagger |0\rangle, \quad (39)$$

i.e., a^\dagger and b^\dagger act just like the fermion creation operators c_\uparrow^\dagger and c_\downarrow^\dagger in this case. The difference between fermion creation and Schwinger boson creation operators shows up only when two (or more) creation operators act on the same site or orbital. The fermion operators create an antisymmetric (or singlet) configuration (in accordance with the Pauli principle),

$$|0, 0\rangle = c_\uparrow^\dagger c_\downarrow^\dagger |0\rangle, \quad (40)$$

while the Schwinger bosons create a totally symmetric (triplet, or higher spin if we create more than two bosons) configuration,

$$\begin{aligned} |1, 1\rangle &= \frac{1}{\sqrt{2}} (a^\dagger)^2 |0\rangle, \\ |1, 0\rangle &= a^\dagger b^\dagger |0\rangle, \\ |1, -1\rangle &= \frac{1}{\sqrt{2}} (b^\dagger)^2 |0\rangle. \end{aligned} \quad (41)$$

To generate the $S = 1$ ground state (27), we first rewrite (2) in terms of Schwinger bosons,

$$\begin{aligned} |\psi_0^{\text{HS}}\rangle &= \sum_{\{z_1, \dots, z_M\}} \psi_0^{\text{HS}}[z] S_{z_1}^+ \cdots S_{z_M}^+ |\downarrow \downarrow \cdots \downarrow\rangle \\ &= \sum_{\{z_1, \dots, z_M; w_1, \dots, w_M\}} \psi_0^{\text{HS}}[z] a_{z_1}^+ \cdots a_{z_M}^\dagger b_{w_1}^+ \cdots b_{w_M}^\dagger |0\rangle \\ &\equiv \Psi_0^{\text{HS}}[a^\dagger, b^\dagger] |0\rangle, \end{aligned} \quad (42)$$

where $M = \frac{N}{2}$ and the w_k 's are those lattice sites which are not occupied by any of the z_i 's. Then the Pfaffian state (29) with (27) is up to an overall normalization factor given by

$$|\psi_0^{S=1}\rangle = \left(\Psi_0^{\text{HS}}[a^\dagger, b^\dagger] \right)^2 |0\rangle. \quad (43)$$

To verify (43), use the identity

$$\begin{aligned} \mathcal{S} \left\{ \prod_{\substack{i,j=1 \\ i < j}}^M (z_i - z_j)^2 \prod_{\substack{i,j=M+1 \\ i < j}}^{2M} (z_i - z_j)^2 \right\} \\ = \text{Pf} \left(\frac{1}{z_i - z_j} \right) \prod_{i < j}^{2M} (z_i - z_j), \end{aligned} \quad (44)$$

where \mathcal{S} indicates symmetrization over all the variables in the curly brackets, and

$$\frac{1}{\sqrt{2}} (a^\dagger)^n (b^\dagger)^{(2-n)} |0\rangle = (\tilde{S}^+)^n |1, -1\rangle, \quad (45)$$

which is readily verified with (35), (41), and the definition (30). To prove (44), use the following identity due to Frobenius⁷²,

$$\begin{aligned} \det \left(\frac{1}{z_i - z_{M+j}} \right) \\ = (-1)^{\frac{M(M+1)}{2}} \frac{\prod_{\substack{i,j=1 \\ i < j}}^M (z_i - z_j) \prod_{\substack{i,j=M+1 \\ i < j}}^{2M} (z_i - z_j)}{\prod_{i=1}^M \prod_{j=M+1}^{2M} (z_i - z_j)}. \end{aligned} \quad (46)$$

The projective construction directly reveals that the state (29) with (27) inherits several symmetries from the Gutzwiller state (translational, $\text{SU}(2)$ spin rotation, parity, and time reversal).

C. Topological degeneracies and non-Abelian statistics

It is well established that $2n$ spatially well separated quasiparticle excitations or vortices carrying half of a

Dirac flux quanta each in the non-Abelian quantized Hall state described by the Pfaffian^{3,4,73} will span an internal or topological Hilbert space of dimensions 2^n (2^{n-1} for either even or odd fermion numbers)⁷⁴, in accordance with the existence of one Majorana fermion state at each vortex core^{5-7,34}. The Majorana fermion states can only be manipulated through braiding of the vortices, with the interchanges being non-commutative or non-Abelian^{2,3,6}.

The question we wish to address in this paper is whether there is any manifestation of this topological space of dimension 2^n , or the $2n$ Majorana fermion states, in the spinon excitation Hilbert space suggested by the $S = 1$ ground state (27). In Section IIB, we have seen that the fractional statistics of the spinons in the Haldane–Shastry model, and presumably in any model supporting one-dimensional anyons, is encoded in the momentum spacings of the excitations. This is not too surprising, as there are no other suitable quantum numbers, like the relative angular momentum for two-dimensional anyons, available. We will propose now that the topological degeneracies, or the occupation numbers of the n fermions consisting of the $2n$ Majorana fermions, are once again encoded in the momentum spacings between single spinon states.

In the Haldane–Shastry model, the spacings between neighboring momenta were always half integer, in accordance with half-Fermi statistics, as the difference between consecutive spinon momentum numbers a_i was always an odd integer,

$$a_{i+1} - a_i = \text{odd}. \quad (47)$$

This follows directly from the construction of the extended Young tableaux illustrated in Fig. 4. When two spinons are in neighboring columns, the difference of the a_i is one and hence an odd integer; when we insert complete columns without spinons in between, the number of boxes we insert is always even.

We will now show that for the $S = 1$ chain with the Hilbert space parameterized by the ground state $|\psi_0^{S=1}\rangle$ and all spinon excitations above it, the corresponding rule is

$$\begin{aligned} a_{i+1} - a_i &= \text{even or odd}, & \text{for } i \text{ odd}, \\ a_{i+1} - a_i &= \text{odd}, & \text{for } i \text{ even}. \end{aligned} \quad (48)$$

As $i = 1, 2, \dots, 2n$, we have a total of n spacings which can be either even or odd, and another n spacings which are always odd. With the single spinon momenta given by

$$p_i = \frac{\pi}{N} \left(a_i - \frac{1}{2} \right), \quad (49)$$

this yields momentum spacings which can be either an integer or an half-integer times $\frac{2\pi}{N}$ for i odd. This is a topological distinction—for Abelian anyons, one choice corresponds to bosons or fermions (which, for most purposes, are equivalent in one dimension), and the other

$$\begin{aligned}
\underbrace{\begin{array}{|c|c|} \hline 1 & 1 \\ \hline 2 & 2 \\ \hline \end{array}} \otimes \underbrace{\begin{array}{|c|c|} \hline 2 & 2 \\ \hline \end{array}} \otimes \underbrace{\begin{array}{|c|c|} \hline 3 & 3 \\ \hline \end{array}} &= \underbrace{\begin{array}{|c|c|c|} \hline 1 & 1 & 3 & 3 \\ \hline 2 & 2 & \bullet & \bullet \\ \hline \end{array}}_{S=1} \oplus \underbrace{\begin{array}{|c|c|c|} \hline 1 & 1 & 2 & \bullet \\ \hline \bullet & 2 & 3 & 3 \\ \hline \end{array}}_{S=0} \oplus \underbrace{\begin{array}{|c|c|c|} \hline 1 & 1 & 2 & 3 \\ \hline \bullet & 2 & 3 & \bullet \\ \hline \end{array}}_{S=1} \oplus \underbrace{\begin{array}{|c|c|c|c|} \hline 1 & 1 & 2 & 3 & 3 \\ \hline \bullet & 2 & \bullet & \bullet & \bullet \\ \hline \end{array}}_{S=2} \oplus \underbrace{\begin{array}{|c|c|c|} \hline 1 & 1 & 2 & 2 \\ \hline \bullet & \bullet & 3 & 3 \\ \hline \end{array}}_{S=1} \oplus \underbrace{\begin{array}{|c|c|c|c|} \hline 1 & 1 & 2 & 2 & 3 \\ \hline \bullet & \bullet & \bullet & \bullet & 3 \\ \hline \end{array}}_{S=2} \oplus \underbrace{\begin{array}{|c|c|c|c|c|} \hline 1 & 1 & 2 & 2 & 3 & 3 \\ \hline \bullet & \bullet & \bullet & \bullet & \bullet & \bullet \\ \hline \end{array}}_{S=3} \\
= \underbrace{\begin{array}{|c|c|} \hline 1 & 1 \\ \hline 2 & 2 \\ \hline \end{array}} \oplus \underbrace{\begin{array}{|c|c|} \hline 1 & 1 & 2 \\ \hline \bullet & 2 & \bullet \\ \hline \end{array}} \\
\oplus \underbrace{\begin{array}{|c|c|c|} \hline 1 & 1 & 2 & 2 \\ \hline \bullet & \bullet & \bullet & \bullet \\ \hline \end{array}}
\end{aligned}$$

FIG. 5. Total spin representations of three $S = 1$ spins in terms of extended Young tableaux.

choice to half-fermions. For spinons which are well separated in momentum space, the states spanning this in total 2^n dimensional topological Hilbert space become degenerate as we approach the thermodynamic limit.

To derive (48), we introduce a second formalism of extended Young tableaux, this time for spin $S = 1$. The general rule we wish to propose for obtaining the tableaux is illustrated in Fig. 5 for three spins with $S = 1$. The construction is as follows. For each of the N spins, put a row of two adjacent boxes, which is equivalent to the Young tableau for a single spin without any numbers in the boxes. Put these N small tableaux on a line and number them consecutively from left to right, with the same number in each pair of boxes which represent a single spin. To obtain the product of some extended Young tableau representing spin S_0 on the left with a spin 1 tableau (i.e., a row of two boxes with the same number in it) on the right, we follow the rule

$$\mathbf{S}_0 \otimes \mathbf{1} = \begin{cases} \mathbf{1}, & \text{for } S_0 = 0, \\ \mathbf{S}_0 - \mathbf{1} \oplus \mathbf{S}_0 \oplus \mathbf{S}_0 + \mathbf{1}, & \text{for } S_0 = 1, 2, \dots \end{cases} \quad (50)$$

i.e., we obtain only one new tableau with both boxes from the right added to the top row if the tableau on the left is a singlet, and three new tableaux if it has spin one or higher. These three tableaux are constructed by adding both boxes to the bottom row (resulting in a representation $\mathbf{S}_0 - \mathbf{1}$), by adding the first box to the bottom row and the second box to the top row without stacking them on top of each other (resulting in a representation \mathbf{S}_0), and by adding both boxes to the top row (resulting in a representation $\mathbf{S}_0 + \mathbf{1}$). In each extended tableau, the boxes must be arranged such that the numbers are strictly increasing in each column from top to bottom, and that they are not decreasing from left to right in that the smallest number in each column cannot be smaller than the largest number in the column to the left of it. In analogy to the case of the Haldane–Shastry model, the empty spaces in between the boxes are filled with dots representing spinons. The spinon momentum number a_i associated with each spinon is given by the number in the box in the same column. A complete table of all the extended Young tableaux for four $S = 1$ spins is shown in Fig. 6. The assignment of physical single spinon momenta to the spinon momentum numbers (49) is identical to this assignment for the Haldane–Shastry model, as we can obtain the 3^N states of the $S = 1$ Hilbert space by

Schwinger boson projection (i.e., by projecting on spin $S = 1$ on each site) from states contained in the $2^N \times 2^N$ dimensional Hilbert space of two $S = \frac{1}{2}$ models, a projection which commutes with the total momentum. The correctness of this assignment has further been verified numerically up to $N = 16$ sites³².

With the tableau structure thus in place, all that is left to show is that the allowed momentum spacings obey (48). Looking at any of the tableaux in Fig. 6, we note that from left to right, the spinons alternate between being assigned to the first of the two boxes with a given number and being assigned to the second of such two boxes. This follows simply from the fact that the number of boxes in between the columns with the two neighboring spinons must be even. The first spinon momentum number a_1 is always odd, but all the other a_i 's can be either even or odd. The rule is therefore that if i is odd, the i -th spinon is assigned to the first of the two boxes with number a_i , and the momentum spacing $a_{i+1} - a_i$ can be either even or odd,

$$\begin{array}{ccc} \begin{array}{|c|c|} \hline 3 & 3 \\ \hline \bullet & \bullet \\ \hline \end{array} & \text{or} & \begin{array}{|c|c|c|} \hline 3 & 3 & 4 \\ \hline \bullet & 4 & \bullet \\ \hline \end{array} & \text{or} & \begin{array}{|c|c|c|c|} \hline 3 & 3 & 4 & 5 \\ \hline \bullet & 4 & 5 & \bullet \\ \hline \end{array} & \text{or} & \dots \\ \text{even} & & \text{odd} & & \text{even} & & \end{array}$$

If i is even, however, the i -th spinon is assigned to the second of the two boxes with number a_i , and the momentum spacing $a_{i+1} - a_i$ has to be odd, as we can insert only an even number of columns between the two spinons (recall that we cannot stack two boxes with the same number in it on top of each other):

$$\begin{array}{ccc} \begin{array}{|c|c|} \hline 3 & 4 \\ \hline \bullet & \bullet \\ \hline \end{array} & \text{or} & \begin{array}{|c|c|c|c|} \hline 3 & 4 & 4 & 6 \\ \hline \bullet & 5 & 5 & \bullet \\ \hline \end{array} & \text{or} & \begin{array}{|c|c|c|c|c|c|} \hline 3 & 4 & 4 & 6 & 6 & 8 \\ \hline \bullet & 5 & 5 & 7 & 7 & \bullet \\ \hline \end{array} & \text{or} & \dots \\ \text{odd} & & \text{odd} & & \text{odd} & & \end{array}$$

The spacings between the single spinon momenta are hence as stated in (48).

IV. TOPOLOGICAL MOMENTUM SPACINGS FOR SU(2) LEVEL k ANYONS IN GENERAL

A. Generalization of the model to arbitrary spin S

The projective generation introduced in Section III B can be generalized to arbitrary spin $S = s$:

$$|\psi_0^S\rangle = \left(\Psi_0^{\text{HS}} [a^\dagger, b^\dagger] \right)^{2s} |0\rangle. \quad (51)$$

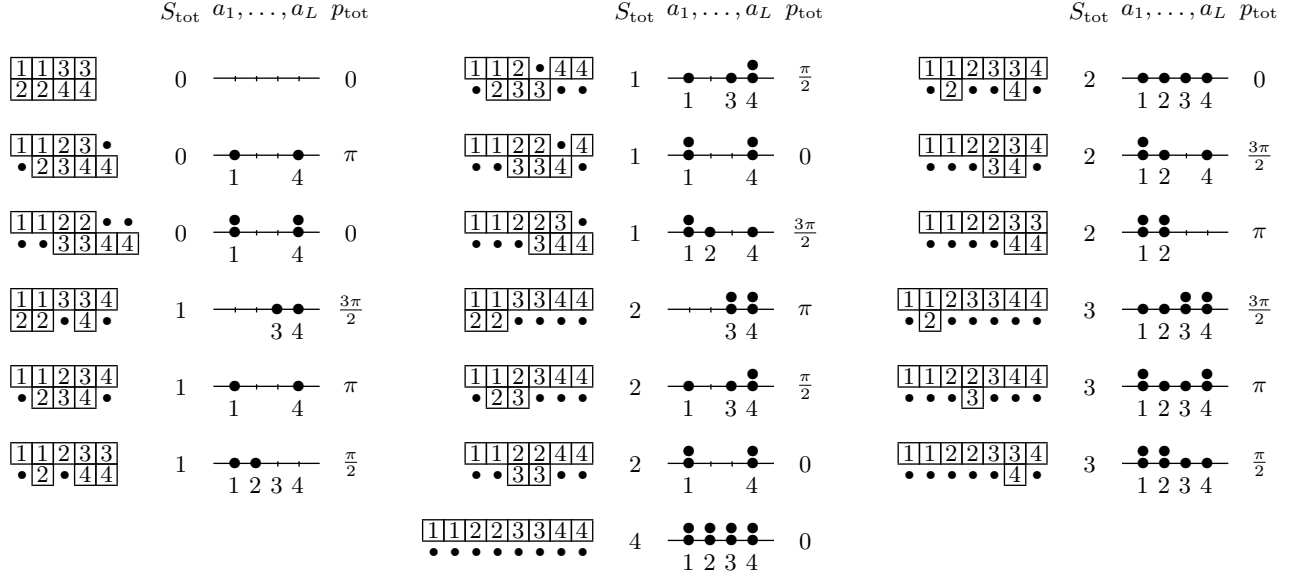


FIG. 6. Extended Young tableau decomposition for an $S = 1$ spin chain with $N = 4$ sites. The dots represent the spinons. The spinon momentum numbers a_i are given by the numbers in the boxes of the same column. Note that $\sum(2S_{\text{tot}} + 1) = 3^N$.

In order to write this state in a form similar to (27)–(31),

$$|\psi_0^S\rangle = \sum_{\{z_1, \dots, z_{sN}\}} \psi_0^S(z_1, \dots, z_{sN}) \tilde{S}_{z_1}^+ \cdots \tilde{S}_{z_{sN}}^+ | -s \rangle_N, \quad (52)$$

where

$$| -s \rangle_N \equiv \otimes_{\alpha=1}^N |s, -s\rangle_{\alpha} \quad (53)$$

is the “vacuum” state in which all the spins are maximally polarized in the negative \hat{z} -direction, we introduce re-normalized spin flip operators \tilde{S}^+ which satisfy

$$\frac{1}{\sqrt{(2s)!}} (a^\dagger)^n (b^\dagger)^{(2s-n)} |0\rangle = (\tilde{S}^+)^n |s, -s\rangle. \quad (54)$$

If we assume a basis in which S^z is diagonal, we may write

$$\tilde{S}^+ \equiv \frac{1}{b^\dagger b + 1} a^\dagger b = \frac{1}{s - S^z + 1} S^+. \quad (55)$$

The wave function for the spin S state (51) is then given by

$$\psi_0^S(z_1, \dots, z_{sN}) = \prod_{m=1}^{2s} \left(\prod_{\substack{i,j=(m-1)M+1 \\ i < j}}^{mM} (z_i - z_j)^2 \right) \prod_{i=1}^{sN} z_i. \quad (56)$$

where $M = \frac{N}{2}$. Note that these states are similar to the Read-Rezayi states¹⁰ in the quantized Hall effect.

As for the $S = 1$ state discussed in Section III B, the projective construction (51) directly implies several symmetries. The state $|\psi_0^S\rangle$ is translationally invariant with ground state momentum $p_0 = -\pi NS$, a spin singlet, and real.

It was again shown by one of us²² that (51) (or (52) with (56)) is the exact ground state of the Hamiltonian

$$H^S = \frac{2\pi^2}{N^2} \left[\sum_{\alpha \neq \beta} \frac{\mathbf{S}_\alpha \mathbf{S}_\beta}{|\eta_\alpha - \eta_\beta|^2} - \frac{1}{2(s+1)(2s+3)} \sum_{\substack{\alpha, \beta, \gamma \\ \alpha \neq \beta, \gamma}} \frac{(\mathbf{S}_\alpha \mathbf{S}_\beta)(\mathbf{S}_\alpha \mathbf{S}_\gamma) + (\mathbf{S}_\alpha \mathbf{S}_\gamma)(\mathbf{S}_\alpha \mathbf{S}_\beta)}{(\bar{\eta}_\alpha - \bar{\eta}_\beta)(\eta_\alpha - \eta_\gamma)} \right], \quad (57)$$

with energy eigenvalue

$$E_0^S = -\frac{\pi^2}{6} \frac{s(s+1)^2}{2s+3} \left(N + \frac{5}{N} \right). \quad (58)$$

Note that the Haldane–Shastry Hamiltonian (1) and the $S = 1$ Hamiltonian (32) are just special cases of this general model.

B. Momentum spacings and topological degeneracies

In Section III C, we have shown that the non-Abelian statistics of the Pfaffian state (27), and in particular the topological degeneracies associated with the Majorana fermion states, manifests itself in topological choices for the (kinematic) momentum spacings of the spinon excitations above the $S = 1$ ground state (27). Specifically, we found that if we label the single spinon momenta in ascending order by $p_i < p_{i+1}$, the spacings $p_{i+1} - p_i$ can be either even or odd multiples of $\frac{\pi}{N}$ if i is odd, while it has to be an odd multiple if i is even.

In this Section, we formulate the corresponding restrictions for the general spin S chain with ground state (51). We will first state the rules and then motivate them. Recall that spinons are represented by dots placed in the empty spaces of extended Young tableaux, and that the momentum number a_i of spinon i is given by the number in the box it shares a column with. For general spin S , the tableau describing the representation on each site is given by

$$\underbrace{\begin{array}{|c|c|c|c|} \hline & & & \\ \hline \end{array}}_{2S \text{ boxes}},$$

i.e., a horizontal array of $2S$ boxes indicating symmetrization, which all contain the same number.

If this number is n , the spinons we assign to any of these boxes will have momentum number $a_i = n$. Let us denote the number of the box a given spinon i with momentum number a_i is assigned to, by b_i , such that box number $b_i = 1$ corresponds to the first, and box number $b_i = 2S$ to the last box with number n in it:

$$\begin{array}{ccc} \begin{array}{|c|c|c|c|} \hline \bullet & & & \\ \hline \end{array} & \begin{array}{|c|c|c|c|} \hline & \bullet & & \\ \hline \end{array} & \dots & \begin{array}{|c|c|c|c|} \hline & & & \bullet \\ \hline \end{array} \\ b_i = 1 & b_i = 2 & & b_i = 2S \end{array}$$

We will see below that if a representation of a spin S chain with L spinons is written in terms of an extended Young tableau, the first spinon with momentum number a_1 will always have box number $b_1 = 1$, and the last spinon with a_L will have $b_L = 2S$. The restrictions corresponding to the non-Abelian (SU(2) level $k = 2S$) statistics of the spinons are described by the flow diagram of the numbers b_i shown in Figure 7.

Let us elaborate this diagram first for the case $S = 1$, which we have already studied in Section III C. In this case,

$$b_i = \begin{cases} 1, & \text{for } i \text{ odd,} \\ 2, & \text{for } i \text{ even.} \end{cases} \quad (59)$$

For i odd, we may move from $b_i = 1$ to $b_{i+1} = 2$ either via the horizontal arrow or via the semicircle in Figure 7a, and $a_{i+1} - a_i$ may hence be either even or odd, respectively. For i even or $b_i = 2$, however, the semicircle is the only available continuation, which implies that the spacing $a_{i+1} - a_i$ must be odd.

For general S , Figure 7b implies that the spacings can be even or odd until $b_i = 2S$ is reached, which is then followed by an odd integer spacing $a_{i+1} - a_i$, as the semicircular arrow is the only possible continuation at this point. Note that for $S \geq 1$, the minimal number of spinons is two (these two spinons then have an odd integer spacing $a_2 - a_1$), and that we cannot have more than $2S$ spinons with the same momentum number $a_i = n$, as $a_{i+1} - a_i = 0$ is even.

We will now motivate this diagram. To begin with, we generalize the formalism of extended Young tableaux to arbitrary spin S . The construction is similar to the one for $S = 1$ outlined in Section III C. For each of the N spins, put a row of $2S$ adjacent boxes. Put these N tableaux on a line and number them consecutively from left to right, with the same number in each row of $2S$ boxes representing a single spin. To obtain the product of some extended Young tableau representing spin S_0 on the left with a spin S tableau (i.e., a row of $2S$ boxes with the same number in it) on the right, we first recall

$$\mathbf{S}_0 \otimes \mathbf{S} = |\mathbf{S}_0 - \mathbf{S}| \oplus |\mathbf{S}_0 - \mathbf{S}| + 1 \oplus \dots \oplus \mathbf{S}_0 + \mathbf{S}, \quad (60)$$

which implies that we obtain either $2S_0 + 1$ or $2S + 1$ new tableaux, depending on which number is smaller. In terms of extended Young tableaux, (60) translates into

$$\begin{array}{l} \begin{array}{|c|} \hline \lrcorner \\ \hline \end{array} \otimes \underbrace{\begin{array}{|c|c|c|c|} \hline n & n & & n \\ \hline \end{array}}_{2S \text{ boxes}} \\ \mathbf{S}_0 \\ = \begin{array}{|c|c|c|c|} \hline \bullet & & & \\ \hline n & n & & n \\ \hline \end{array} \oplus \begin{array}{|c|c|c|c|} \hline \bullet & & & n \\ \hline n & n & & \\ \hline \end{array} \oplus \begin{array}{|c|c|c|c|} \hline & & & n \\ \hline n & & & n \\ \hline \end{array} \\ \text{for } S_0 \geq S \quad \text{for } S_0 \geq S - \frac{1}{2} \quad \text{for } S_0 \geq S - 1 \\ \oplus \dots \\ \oplus \begin{array}{|c|c|c|c|} \hline \bullet & & & n \\ \hline n & n & & \\ \hline \end{array} \oplus \begin{array}{|c|c|c|c|} \hline & \bullet & & n \\ \hline n & & & n \\ \hline \end{array} \oplus \begin{array}{|c|c|c|c|} \hline & & & \bullet \\ \hline n & n & & n \\ \hline \end{array} \\ \text{for } S_0 \geq 1 \quad \text{for } S_0 \geq \frac{1}{2} \quad \text{always} \end{array} \quad (61)$$

The first tableau on the right-hand side of (61) exists only for $S_0 \geq S$, the second only for $S_0 \geq S - \frac{1}{2}$, and

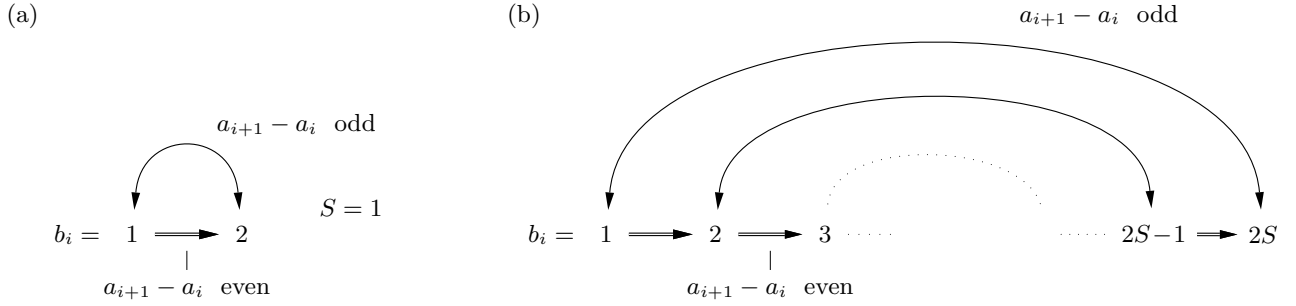


FIG. 7. Non-Abelian (SU(2) level $k = 2S$) statistics in one dimension: flow diagram for the (auxiliary) box numbers b_i , which serve to describe the restrictions for the spinon momentum number spacings $a_{i+1} - a_i$ for the critical models of spin chains introduced in Sections III A and IV A with (a) $S = 1$, and (b) general spin S . The unidirectional, horizontal arrows correspond to even integer momentum number spacings $a_{i+1} - a_i$, while the bidirectional, semicircle arrows correspond to odd integer spacings.

so on. Note that the shape of the right boundary of the extended Young tableaux for \mathcal{S}_0 does not determine which tableaux are contained in the expansion of $\mathcal{S}_0 \otimes \mathcal{S}$, as this depends only on the number $S_0 - S$. In the expansion (61), the $2S$ boxes representing a single spin S always reside in adjacent columns. In an extended tableau, the numbers in the boxes are equal or increasing as we go from left to right, and strictly increasing from top to bottom. The empty spaces we obtain as we build up the tableaux via this method represent the spinons. Note that we cannot take a given tableau and just add a pair of spinons by inserting them somewhere, as the resulting tableau would not occur in the expansion.

In Figure 8, we illustrate the principle by writing out a few terms in the expansion for an $S = 2$ chain. We now turn to the question what this construction implies for the momentum spacings of the spinons. It is very easy to see from Figure 8 that $b_1 = 1$ and a_1 is odd, and that $b_L = 2S$ and a_L is even (odd) for N even (odd). Let us assume we have a spinon i with momentum number a_i and box number b_i . If we take $S = 3$, $a_i = 3$, and $b_i = 2$, this spinon would be represented by a dot which shares a column with the second box with number 3 in it,

$$\begin{array}{c} \boxed{3333333} \\ \bullet \\ b_i = 2 \end{array}$$

For the box number b_{i+1} of the next spinon, there are only two possibilities:

(i) $b_{i+1} = b_i + 1$, which implies that $a_{i+1} - a_i$ is even. The spinons either sit in neighboring columns with $a_{i+1} = a_i$, or contain an even number of spin S representations (with $2S$ boxes each) in between them. For our example, the corresponding tableaux are

$$\begin{array}{c} \boxed{3333333} \\ \bullet \\ b_i \quad b_{i+1} \\ a_{i+1} = a_i \end{array} \quad \text{and} \quad \begin{array}{c} \boxed{333333344455555} \\ \bullet \\ b_i \quad b_{i+1} \\ a_{i+1} = a_i + 2 \end{array} \quad \text{and} \quad \dots$$

This possibility produces the unidirectional, horizontal arrows in Figure 7. If $b_i = 2S$, this possibility does not exist, and there are either no further spinons or $a_{i+1} - a_i$ has to be odd.

(ii) $b_{i+1} = 2S - b_i + 1$, which implies that $a_{i+1} - a_i$ is odd. For our example, the tableaux are

$$\begin{array}{c} \boxed{3333333444} \\ \bullet \\ b_i \quad b_{i+1} \\ a_{i+1} = a_i + 1 \end{array} \quad \text{and} \quad \begin{array}{c} \boxed{33333334445555666} \\ \bullet \\ b_i \quad b_{i+1} \\ a_{i+1} = a_i + 3 \end{array} \quad \dots$$

This possibility produces the bidirectional, semicircle arrows in Figure 7.

This concludes the motivation of the flow diagram in Figure 7b. As in Sections II C and III C, the single spinon momenta are given by

$$p_i = \frac{\pi}{N} \left(a_i - \frac{1}{2} \right). \quad (62)$$

This yields momentum spacings $p_{i+1} - p_i$ which can be either an integer or an half-integer times $\frac{2\pi}{N}$.

V. CORRESPONDENCE WITH SU(2) LEVEL k FUSION RULES

In this section, we establish a one-to-one correspondence between the topological choices for the momentum spacings and the fusion rules of spin $\frac{1}{2}$ spinons in the SU(2) level k Wess–Zumino–Witten model^{26,27}. The results we present are completely consistent with, and in many ways complementary to, those obtained by Bouwknegt, Ludwig, and Schoutens^{35–38} based on the Yangian symmetry of the conformal field theory.

The “deformed” Lie algebra SU(2) level k is in essence an SU(2) spin algebra with the maximal spin restricted to $\frac{k}{2}$,

$$j = 0, \frac{1}{2}, 1, \frac{3}{2}, \dots, \frac{k}{2}. \quad (63)$$

$$\begin{aligned}
\begin{array}{c} \boxed{11111} \\ S=2 \end{array} \otimes \begin{array}{c} \boxed{22222} \\ S=2 \end{array} &= \begin{array}{c} \boxed{11111} \\ \boxed{22222} \\ S=0 \end{array} \oplus \begin{array}{c} \boxed{111112} \\ \bullet \boxed{2222} \bullet \\ S=1 \end{array} \oplus \begin{array}{c} \boxed{11111222} \\ \bullet \bullet \bullet \boxed{22} \bullet \bullet \bullet \\ S=2 \end{array} \oplus \begin{array}{c} \boxed{111112222} \\ \bullet \bullet \bullet \bullet \bullet \boxed{2} \bullet \bullet \bullet \bullet \bullet \\ S=3 \end{array} \oplus \begin{array}{c} \boxed{1111122222} \\ \bullet \bullet \bullet \bullet \bullet \bullet \bullet \bullet \bullet \bullet \bullet \bullet \bullet \\ S=4 \end{array} \\
\begin{array}{c} \boxed{11111} \\ \boxed{22222} \\ S=0 \end{array} \otimes \begin{array}{c} \boxed{33333} \\ S=2 \end{array} &= \begin{array}{c} \boxed{1111133333} \\ \boxed{22222} \bullet \bullet \bullet \bullet \bullet \\ S=2 \end{array} \\
\begin{array}{c} \boxed{111112} \\ \boxed{2222} \\ S=1 \end{array} \otimes \begin{array}{c} \boxed{33333} \\ S=2 \end{array} &= \begin{array}{c} \boxed{111112} \bullet \boxed{33} \\ \bullet \bullet \bullet \boxed{222233} \bullet \bullet \bullet \\ S=1 \end{array} \oplus \begin{array}{c} \boxed{1111123333} \\ \bullet \bullet \bullet \boxed{22223} \bullet \bullet \bullet \bullet \bullet \\ S=2 \end{array} \oplus \begin{array}{c} \boxed{11111233333} \\ \bullet \bullet \bullet \boxed{2222} \bullet \bullet \bullet \bullet \bullet \bullet \bullet \\ S=3 \end{array} \\
\begin{array}{c} \boxed{1111122} \\ \boxed{22} \\ S=2 \end{array} \otimes \begin{array}{c} \boxed{33333} \\ S=2 \end{array} &= \begin{array}{c} \boxed{1111122} \bullet \bullet \bullet \\ \bullet \bullet \bullet \boxed{2233333} \\ S=0 \end{array} \oplus \begin{array}{c} \boxed{1111122} \bullet \bullet \bullet \\ \bullet \bullet \bullet \boxed{223333} \bullet \\ S=1 \end{array} \oplus \begin{array}{c} \boxed{1111122333} \\ \bullet \bullet \bullet \boxed{22333} \bullet \bullet \bullet \\ S=2 \end{array} \oplus \begin{array}{c} \boxed{11111223333} \\ \bullet \bullet \bullet \boxed{22} \bullet \bullet \bullet \bullet \bullet \bullet \bullet \bullet \bullet \\ S=3 \end{array} \\
&\oplus \begin{array}{c} \boxed{11111223333} \\ \bullet \bullet \bullet \boxed{22} \bullet \bullet \bullet \bullet \bullet \bullet \bullet \bullet \bullet \\ S=4 \end{array}
\end{aligned}$$

FIG. 8. Examples of products of extended tableaux for an $S = 2$ spin chain.

The fusion rules, and also the only possible rules consistent with associativity, are given by

$$\begin{aligned}
j_1 \otimes j_2 &= |j_1 - j_2| \oplus |j_1 - j_2| + 1 \oplus \dots \\
&\dots \oplus \min\{j_1 + j_2, k - j_1 - j_2\}. \quad (64)
\end{aligned}$$

We will now investigate what these fusion rules imply for the spinons of the models studied in the previous sections.

We begin with the Haldane–Shastry chain, which is a microscopic lattice realization of the $SU(2)$ level $k = 1$ Wess-Zumino-Witten model. For $k = 1$, the relevant fusion rules (64) are

$$\begin{aligned}
0 \otimes \frac{1}{2} &= \frac{1}{2}, \\
\frac{1}{2} \otimes \frac{1}{2} &= 0, \quad (65)
\end{aligned}$$

i.e., the fusion of two representations always yields a unique representation. The fusion diagram we obtain as we combine, starting from $j = 0$, spinons with $j = \frac{1}{2}$, is likewise unique, as illustrated in Figure 9a. In the case of the Haldane–Shastry model, the momentum spacings $a_{i+1} - a_i$ of the spinons are always odd, in accordance with Abelian half-Fermi statistics, a result we ultimately wish to relate to the fusion diagram.

We now turn to the $S = 1$ model discussed in Section III. The relevant fusion rules for $k = 2$ are

$$\begin{aligned}
0 \otimes \frac{1}{2} &= \frac{1}{2}, \\
\frac{1}{2} \otimes \frac{1}{2} &= 0 \oplus 1, \\
1 \otimes \frac{1}{2} &= \frac{1}{2}, \quad (66)
\end{aligned}$$

i.e., whenever we reach a representation $j = \frac{1}{2}$ on a horizontal link in the fusion diagram, we have a choice between obtaining $j = 0$ or $j = 1$ when fusing it with the next spinon on the right, as illustrated in Figure 9b. Since we reach $j = \frac{1}{2}$ after every second spinon, the number of choices we obtain is completely equivalent to the number we obtained via the extended Young tableau formalism in Section III C (see also Figure 7b). With this formalism, we further established that the momentum spacing $a_{i+1} - a_i$ is odd whenever fusing the previous spinon does not allow for a choice, and may be either even or odd whenever the previous fusion provided us with a choice.

We may hence tentatively assume that, whenever the direction of the declining or ascending lines in the lower diagram in Figure 9b changes, the spacing $a_{i+1} - a_i$ between the two spinons on both sides is odd (as for Abelian half-Fermi statistics), and that whenever the direction of the line does not change, the spacing $a_{i+1} - a_i$ is even (as for Abelian Bose or Fermi statistics).

We will now confirm this assumption by elaborating the case of the general spin S model discussed in Section IV. The spinons of this model obey non-Abelian $SU(2)$ level $k = 2S$ statistics. The relevant fusion rules are

$$\begin{aligned}
0 \otimes \frac{1}{2} &= \frac{1}{2}, \\
j \otimes \frac{1}{2} &= j - \frac{1}{2} \oplus j + \frac{1}{2}, \quad \text{for } 0 < j < S, \\
S \otimes \frac{1}{2} &= S - \frac{1}{2}, \quad (67)
\end{aligned}$$

i.e., unless $j = 0$ or $j = S$ on a horizontal link in the fusion diagram, we have a choice of two possible representations when we fuse j with the next spinon, as illustrated in Figure 9c. Each line in the lower diagram of

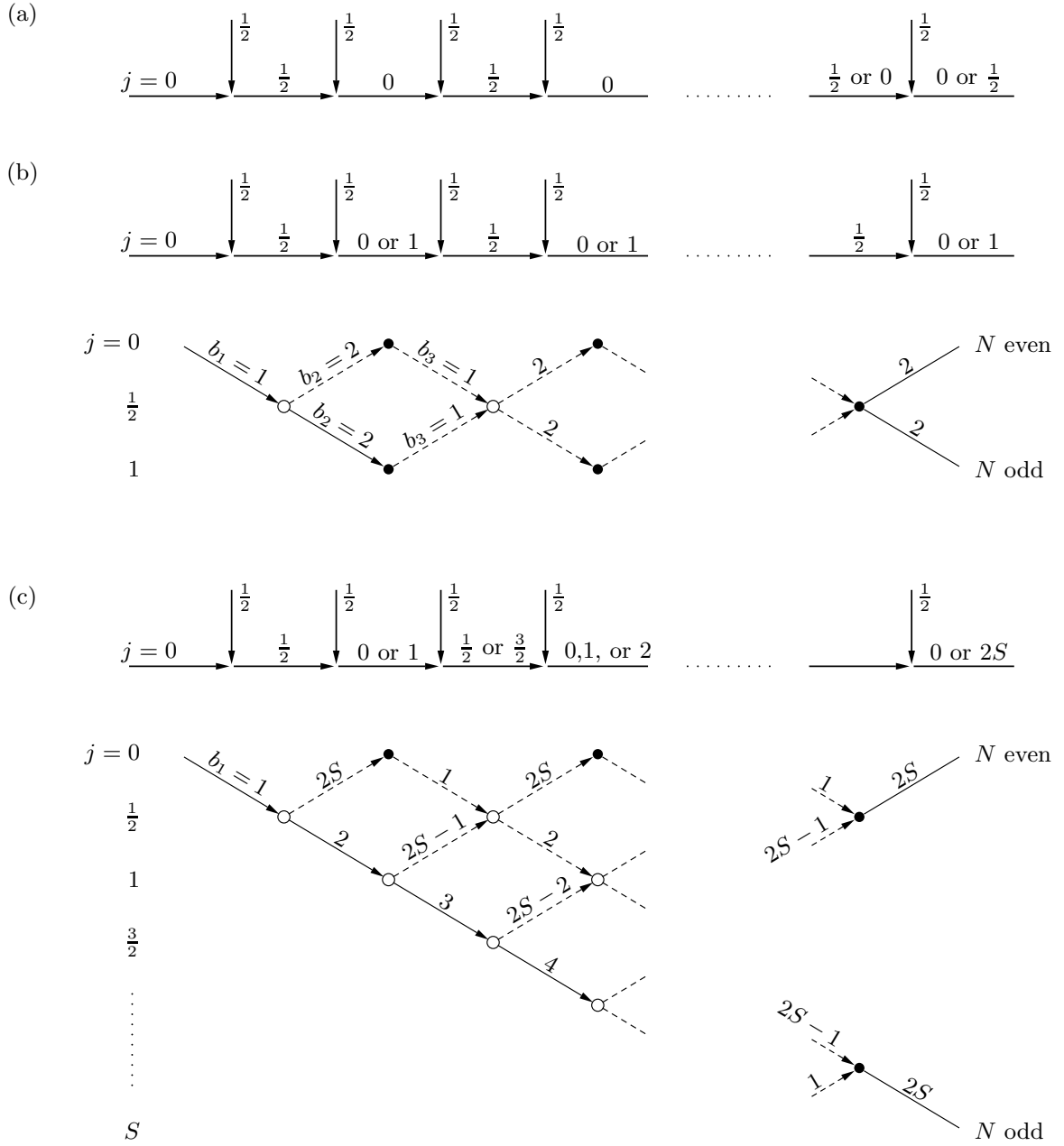


FIG. 9. Fusion trees and Bratteli diagrams for $SU(2)$ level $k = 2S$ spinons: (a) In the Haldane–Shastry model ($k = 1$), there is only one possible fusion trajectory for spinons with $j_i = \frac{1}{2}$, with j on the links alternating between 0 and $\frac{1}{2}$. The momentum spacings $a_{i+1} - a_i$ are always odd. (b) For the critical $S = 1$ model studied in Section III, the fusion rules (64) for Ising anyons ($k = 2$) allow for a choice whenever we reach $j = \frac{1}{2}$, which is the case after every other spinon. The momentum spacings $a_{i+1} - a_i$ are odd when we do not have a choice, and either even or odd when we have a choice. (c) In the general $k = 2S$ model studied in Section IV, there are many possible fusion trajectories, as illustrated by the dotted lines in the lower diagram. We have a choice between two possibilities at all points where j reaches neither 0 nor S . Continuation in the same direction, as illustrated for the first four spinons with a solid line, corresponds to following the unidirectional, horizontal arrows in Figure 7b, which implies that $b_{i+1} = b_i + 1$ and that $a_{i+1} - a_i$ is even. Changing direction via a kink, on the other hand, corresponds to following one of the bidirectional, semicircle arrows in Figure 7b, and implies that $b_{i+1} = 2S + 1 - b_i$ and that $a_{i+1} - a_i$ is odd.

this figure represents a spinon, and each dot on its left represents the fusion of this spinon with the representation j from all the previous spinons. The numbers on the

declining or ascending lines denote the box numbers b_i of the spinons, which are assigned according to the assumption we wish to confirm. As assigned, they are uniquely

determined by the vertical position and directions of the lines in the diagram. Drawn with solid lines on the left of the diagram is the simple sequence $b_1 = 1$, $b_2 = 2$, $b_3 = 3$, $b_4 = 4$, which corresponds to following the horizontal arrows in the flow diagram shown in Figure 7b. This implies that the momentum spacings $a_4 - a_3$, $a_3 - a_2$, and $a_2 - a_1$ are even for this sequence. The dotted lines represent the alternatives. Each time we change the direction of the lines, say from declining to ascending as we add the second spinon, the dot at the kink corresponds to one of the bidirectional, semicircle arrows in Figure 7b. The kinks hence represent even spacings $a_{i+1} - a_i$, as assumed above.

The diagram in Figure 9c shows that there is a very large number of possible trajectories. Unless we have reached $j = 0$ or $j = S$, both of which correspond to the last box $b_i = 2S$ in Figure 7b, we have the choice between continuing in the direction of the line representing the previous spinon i (which implies $a_{i+1} - a_i$ even, as for Abelian Bose or Fermi statistics), or changing the direction (which implies $a_{i+1} - a_i$ odd, as for Abelian half-Fermi statistics).

With the last spinon, we must always reach $b_i = 2S$. If the number of sites N of the chain with PBCs is even, we must conclude with $j = 0$. It is not difficult to see from Figure 9c that the number of spinons must be even in this case. If N is odd, however, we must conclude with $j = S$. The number of spinons is given by $2S$ plus a non-negative, even integer. These restrictions are completely consistent with what we would expect from the projective construction of the wave functions we discussed in Section IV B. If N is odd, we need at least one spinon in each of the $2S$ Haldane–Shastry chains we project together. Further spinons can only be created in pairs.

It is not really surprising that there is a one-to-one correspondence between the fusion rules of $SU(2)$ level $k = 2S$ spinons with $j = \frac{1}{2}$ and the rules for constructing the internal Hilbert space for the $SU(2)$ level $k = 2S$ anyons we have derived in the previous sections. It is instructive, however, as this correspondence provides us with the physical momentum spacings we obtain as we fuse the $j = \frac{1}{2}$ representations of the individual spinons according to the fusion diagram in Figure 9c.

Since the notation of the momentum numbers a_i is tied to the Young tableau formalism introduced in Reference 31 and generalized to higher spin models in the previous sections, it is appropriate to state the rules for the momentum spacings in a generally more familiar language. If we fuse two $SU(2)$ spinons in an $SU(2)$ level $k = 2S$ model (either one of the microscopic models introduced by one of us^{22,23} or the conformal field theory of Wess, Zumino and Witten^{26,27}, with the spinon bases studied by Bouwknegt, Ludwig, and Schoutens^{35–38}) with $j = \frac{1}{2}$ each, and neighboring single spinon momenta p_i and p_{i+1} , the spacing between these two momenta $p_{i+1} - p_i$ is quantized according to Abelian half-Fermi statistics, if and only if there is a kink between the spinons in the

Bratteli diagram,

$$p_{i+1} - p_i = \frac{2\pi\hbar}{L} \left(\frac{1}{2} + \text{integer} \right), \quad (68)$$

where L is the length of the chain with PBCs. (“Neighboring” here means that there are no other spinons with momenta between p_i and p_{i+1}). If, on the other hand, the two spinons form a straight line in the Bratteli diagram, the spacing between the neighboring single spinon momenta p_i and p_{i+1} is quantized according to Bose or Fermi statistics (which are equivalent for our purposes here),

$$p_{i+1} - p_i = \frac{2\pi\hbar}{L} \cdot \text{integer}. \quad (69)$$

These shifts are topological quantum numbers. The spinon states with different shifts become degenerate in the thermodynamic limit, but since the states are topologically different, it is not possible to connect them with local perturbation. The situation here is analogous to the Majorana fermion states in the vortex cores of the quasiparticles of the Moore–Read state.

VI. DOMAIN WALLS IN VALENCE BOND PHASES

One way to understand the $SU(2)$ level k Wess–Zumino–Witten model for a spin chain with spin $S = \frac{k}{2}$ is as a description of the multicritical point between the $k+1$ different “dimerization” or valence bond solid (VBS) phases the spin chain can assume in the ground state. Three of the possible VBS configurations for a chain with spin $S \geq 1$ are shown in Figure 10. Here, the spin S at each site is understood to be formed through the completely symmetric projection of $k = 2S$ spin $\frac{1}{2}$ ’s onto one spin S . Before projection, the constituent spin $\frac{1}{2}$ ’s are arranged into dimers, indicated by the solid, horizontal lines, which are just singlets formed by two spins at neighboring sites on the same constituent chain.

In this framework, single spinon excitations are minimal domain walls between the dimerized phases. In

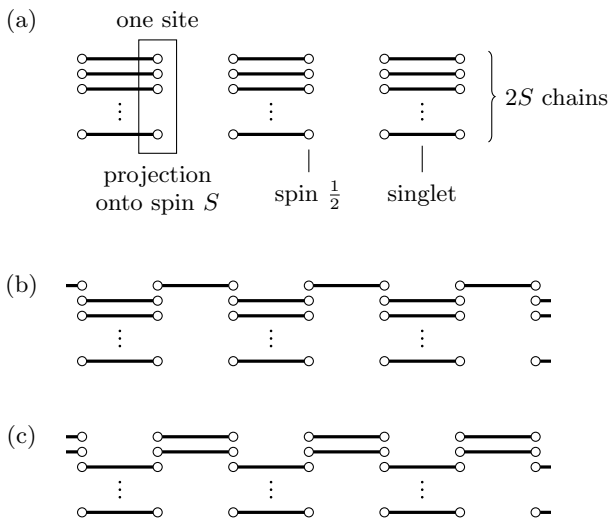


FIG. 10. (a)–(c) Illustration of three of the $2S + 1$ possible dimer configurations for a spin S chain. The spin S at each site of the chain is obtained by symmetric projection of the $k = 2S$ constituent spin $\frac{1}{2}$'s. The different dimerization patterns are obtained from the reference pattern ($j = 0$) shown in (a) by shifting $2j$, $j = 0, \frac{1}{2}, 1, \frac{3}{2}, \dots, S$ of the $2S$ dimerized constituent chains by one lattice spacing. The critical $SU(2)$ level k spin chain can be thought of as the multi-critical point between all the possible dimer phases.

Figure 11, we illustrate the correspondence between the spinons, the labels j from Figure 9, and the Bratteli diagrams with a few examples. Let us first look at Figure 11a. The first spinons shifts the dimer configurations from the initial one, to which we assign label $j = 0$, by one lattice spacing. Following the terminology introduced in Section V, we assign the label $j = \frac{1}{2}$ to the chain where one constituent chain (and in this first example we have only one constituent chain) has shifted by one lattice spacing. If the number of sites on the chain is even, we need an even number of domain walls, and hence an even number of spinons in each constituent chain to close the boundary. This is in correspondence with the Bratteli diagram shown to the right of the chain in Figure 11a. Three of the many, possible spinon configurations for a spin $S = 1$ chain, and the corresponding Bratteli diagrams, are shown in Figures 11b, 11c, and 11d. In these pictures, the distance between spinons on the same constituent chain in units of lattice spacings is an odd number, and an even number for neighboring spinons on different constituent chains. Making the connection with the results of Sections IV B and V, we see that the momentum spacing between neighboring spinons is according to (68) for spinons on the same constituent chain, and according to (69) for spinons on different constituent chains. Periodic chains with an odd number of sites require an odd number of domain walls, and hence an odd number of spinons, on each constituent chain. The minimal number of spinons in this case is $2S$, as illustrated for an $S = 1$ chain in Figure 11c. In Figure 11d, we give

an example indicating how the application of these rules proceeds to chains with general spin S .

Viewing spinons, which are by definitions excitations with spin $\frac{1}{2}$ and no charge (as compared to electrons, which have spin $\frac{1}{2}$ and charge -1 , or spin flips, which carry spin 1 and no charge), as domain walls in dimerized chains is intuitively rewarding. It correctly captures many subtle technical issues like the state counting, and hence to a limited extent also the statistics, even though no information regarding the physical manifestation of the fractional statistics, the fractional shifts in the momentum spacings, can be extracted. That a direct correspondence between the dimer phases and the Bratteli diagrams can be established, however, is remarkable since the chains we describe are critical, and do not display any dimerization patterns. The reason is that we can view the critical, and for $S > \frac{1}{2}$ multicritical, phases of the spin chains as the critical points between all the possible dimer phases. At criticality, quantum fluctuations will have destroyed any possible dimerization in the chains, but—and this is the crucial point—will not have altered the topological properties of the spinon excitations we can visualize as domain walls in dimerized chains. The quantum statistics of the spinons, is among these topological properties. Of course, the spinon excitations in the critical chains are not localized in real space, and do not provide a context to consider neighboring spinons in real space. As we have argued in Section IV B, the good and robust quantum numbers in the critical chains are the topological shifts in the relative spacings between neighboring spinons in momentum space, not in real space.

VII. CONCLUSION

In this article, we have argued that in one dimension, non-Abelian, and in particular $SU(2)$ level k statistics, manifests itself in fractional, topological shifts in the spacings of neighboring quasiparticle momenta $p_{i+1} - p_i$, and derived the general rules which patterns for the shifts are allowed for each k . For $k = 2$, the case of Ising anyons, we found that the state counting of the internal Hilbert space associated with the non-Abelian statistics is equivalent to that of Majorana fermion states attached to the spinons. This led us to refer to the shifts as Majorana spacings. For this case, the braiding of the vortices carrying Majorana fermions in the two dimensional analog, the Pfaffian quantum Hall state, is also well understood⁶. We consider it likely that we can learn something about the open problem of the braiding properties of $SU(2)$ level $k > 2$ vortices in Read–Rezayi states by exploring the analogy to the one dimensional models we studied here.

The most important aspect of the emerging picture is the general validity, which needs some clarification. We have derived the formalism for non-Abelian $SU(2)$ level k statistics using spin chains with spin $S \geq \frac{1}{2}$ tuned to the multicritical point. We found that the quantum statis-

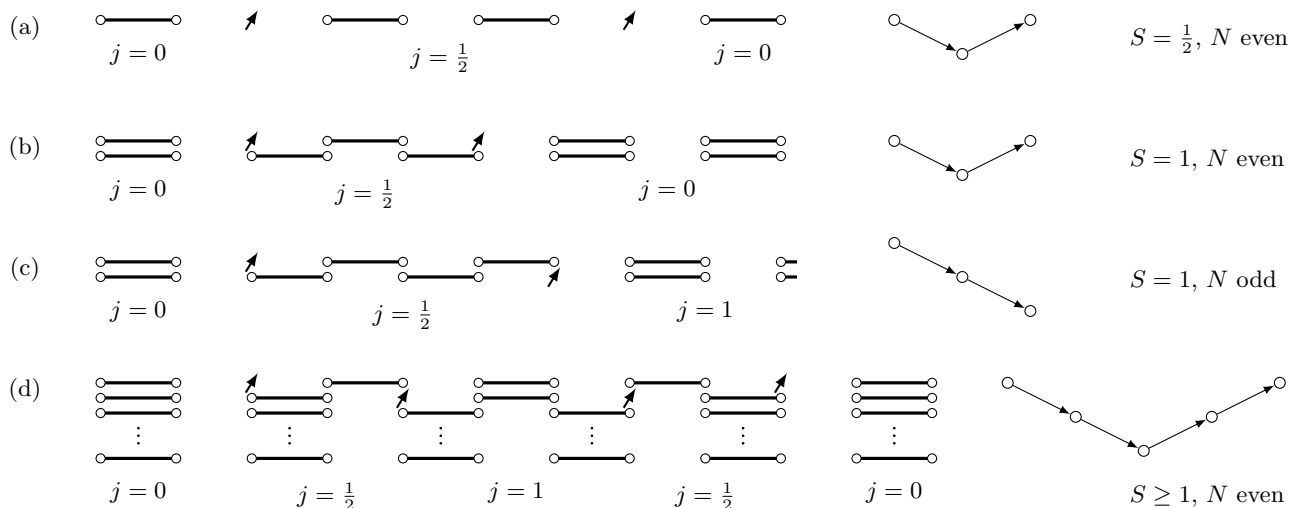


FIG. 11. Examples of dimer configurations with two or four spinon excitations (domain walls) in (a) a spin $\frac{1}{2}$ chain, (b) and (c) a spin 1 chain, and (d) a spin chain with spin $S \geq 1$. The chains are assumed to have periodic boundary conditions and even or odd number of sites N , as indicated. Note that each domain wall shifts one constituent chain by one lattice spacing, and hence changes the configuration label j by $\pm\frac{1}{2}$. It is hence trivial to read off the corresponding Bratteli diagrams, which are depicted to the right of each of the dimerized chains. Note that even though no dimerization occurs in the multi-critical $SU(2)$ level k spin chain we discuss in Sections IV B and V, the Bratteli diagrams, and hence the topological properties (i.e., momentum spacings) of the spinons are nonetheless identical to those of the spinons or domain walls in the dimerized chains.

tics of the spinons in these systems is encoded in the topological shifts in momentum spacings between spinons with neighboring momenta, as detailed in Section IV B. The only case where the individual spinon momenta are known to be perfectly good quantum numbers, however, is the Haldane–Shastry model for spin $\frac{1}{2}$. A natural question to ask, therefore, is what happens in a general, critical or multi-critical, spin chain, when the spinon momenta are not good quantum numbers. Are our results, or is our formalism, still applicable to the general case? Fortunately, the answer is yes. The spacings between the adjacent momenta of the particles carrying the Abelian or non-Abelian, fractional statistics are given by the sum of the topological shifts derived above, and integer spacings which we have not specified. In (68) and (69), the topological shifts are $\frac{1}{2}$ and 0, respectively.

The key point is that while there is no reason to assume that the integers in (68) and (69), are good quantum numbers in a general system, the *topological shifts are always good quantum numbers*.

The situation is comparable to fermions, bosons, and anyons in two space dimensions. There, the relative angular momentum between two identical particles is an odd integer times \hbar for fermions, an even integer times \hbar for bosons, and an even integer plus the statistical parameter θ times \hbar/π for anyons. In a many particle state in two-dimensions, like an electron liquid forming a quantized Hall state or a liquid of quasiparticles with fractional statistics forming a daughter fluid, the relative momentum between two fermions or two anyons is never a good quantum number. The topological shift, that is, the

integer being odd or even for fermions or bosons, respectively, and shifted by θ/π away from bosons for Abelian anyons, however, is always a good quantum number. This shift specifies the (fractional) statistics. Similarly, the momenta of the Abelian and non-Abelian anyons in one space dimension do not have to be good quantum numbers, while the topological shifts to the otherwise integer momentum spacings we derived above, will always be good quantum numbers. These spacings specify the Abelian or non-Abelian statistics, and are topological properties of the $SU(2)$ level k WZW model.

An important, but by contrast unresolved, question is whether the non-Abelian statistics of the one-dimensional models, if realized in a multi-critical spin chain in the laboratory, could be used in quantum computation or quantum cryptography. Unfortunately, we have no definite answers to report at the present time.

ACKNOWLEDGMENTS

MG would like to thank Eddy Ardonne for discussions. MG and RT are supported by the DFG through SFB 1170 ToCoTronics (project B04), and further acknowledge financial support from the DFG through the Würzburg-Dresden Cluster of Excellence on Complexity and Topology in Quantum Matter – *ct.qmat* (EXC 2147, project-id 39085490). FDMH acknowledges funding from the Princeton Center for Complex Materials, a MRSEC supported by NSF Grant DMR 1420541.

- ¹ F. Wilczek, *Fractional statistics and anyon superconductivity* (World Scientific, Singapore, 1990).
- ² A. Stern, *Nature* **464**, 187 (2010).
- ³ G. Moore and N. Read, *Nucl. Phys. B* **360**, 362 (1991).
- ⁴ M. Greiter, X. G. Wen, and F. Wilczek, *Nucl. Phys. B* **374**, 567 (1992).
- ⁵ N. Read and D. Green, *Phys. Rev. B* **61**, 10267 (2000).
- ⁶ D. A. Ivanov, *Phys. Rev. Lett.* **86**, 268 (2001).
- ⁷ A. Stern, F. von Oppen, and E. Mariani, *Phys. Rev. B* **70**, 205338 (2004).
- ⁸ A. Y. Kitaev, *Ann. Phys.* **303**, 2 (2003).
- ⁹ C. Nayak, S. H. Simon, A. Stern, M. Freedman, and S. Das Sarma, *Rev. Mod. Phys.* **80**, 1083 (2008).
- ¹⁰ N. Read and E. Rezayi, *Phys. Rev. B* **59**, 8084 (1999).
- ¹¹ A. Kitaev, *Ann. of Phys.* **321**, 2 (2006).
- ¹² H. Yao and S. A. Kivelson, *Phys. Rev. Lett.* **99**, 247203 (2007).
- ¹³ H. Yao and D.-H. Lee, *Phys. Rev. Lett.* **107**, 087205 (2011).
- ¹⁴ M. Greiter and R. Thomale, *Phys. Rev. Lett.* **102**, 207203 (2009).
- ¹⁵ B. Scharfenberger, R. Thomale, and M. Greiter, *Phys. Rev. B* **84**, 140404 (2011).
- ¹⁶ M. Greiter, D. F. Schroeter, and R. Thomale, *Phys. Rev. B* **89**, 165125 (2014).
- ¹⁷ T. Meng, T. Neupert, M. Greiter, and R. Thomale, *Phys. Rev. B* **91**, 241106 (2015).
- ¹⁸ P. Lecheminant and A. M. Tsvelik, *Phys. Rev. B* **95**, 140406 (2017).
- ¹⁹ I. Glasser, J. I. Cirac, G. Sierra, and A. E. B. Nielsen, *New Journal of Physics* **17**, 082001 (2015).
- ²⁰ Z.-X. Liu, H.-H. Tu, Y.-H. Wu, R.-Q. He, X.-J. Liu, Y. Zhou, and T.-K. Ng, *Phys. Rev. B* **97**, 195158 (2018).
- ²¹ J. Wildeboer and N. E. Bonesteel, *Phys. Rev. B* **94**, 045125 (2016).
- ²² M. Greiter, *Mapping of Parent Hamiltonians*, Vol. 244 of *Springer Tracts in Modern Physics* (Springer, Berlin/Heidelberg, 2011), published also as [arXiv:1109.6104](https://arxiv.org/abs/1109.6104).
- ²³ A. E. B. Nielsen, J. I. Cirac, and G. Sierra, *J. Stat. Mech.: Theory and Experiment* **11**, P11014 (2011).
- ²⁴ F. D. M. Haldane, *Phys. Rev. Lett.* **60**, 635 (1988).
- ²⁵ B. S. Shastry, *Phys. Rev. Lett.* **60**, 639 (1988).
- ²⁶ J. Wess and B. Zumino, *Phys. Lett.* **37B**, 95 (1971).
- ²⁷ E. Witten, *Commun. Math. Phys.* **92**, 455 (1984).
- ²⁸ P. Di Francesco, P. Mathieu, and D. Sénéchal, *Conformal Field Theory* (Springer, New York, 1997).
- ²⁹ F. D. M. Haldane, *Phys. Rev. Lett.* **67**, 937 (1991).
- ³⁰ M. Greiter, *Phys. Rev. B* **79**, 064409 (2009).
- ³¹ M. Greiter and D. Schuricht, *Phys. Rev. Lett.* **98**, 237202 (2007).
- ³² B. Scharfenberger and M. Greiter, *Journal of Physics A: Mathematical and Theoretical* **45**, 455202 (2012).
- ³³ R. Thomale, S. Rachel, P. Schmitteckert, and M. Greiter, *Phys. Rev. B* **85**, 195149 (2012).
- ³⁴ N. B. Kopnin and M. M. Salomaa, *Phys. Rev. B* **44**, 9667 (1991).
- ³⁵ P. Bouwknegt, A. W. W. Ludwig, and K. Schoutens, *Phys. Lett. B* **338**, 448 (1994).
- ³⁶ P. Bouwknegt, A. W. W. Ludwig, and K. Schoutens, *Phys. Lett. B* **359**, 304 (1995).
- ³⁷ P. Bouwknegt and K. Schoutens, *Nucl. Phys. B* **482**, 345 (1996).
- ³⁸ P. Bouwknegt and K. Schoutens, *Nucl. Phys. B* **547**, 501 (1999).
- ³⁹ I. Affleck, *Nucl. Phys. B* **265**, 409 (1986).
- ⁴⁰ I. Affleck and F. D. M. Haldane, *Phys. Rev. B* **36**, 5291 (1987).
- ⁴¹ F. D. M. Haldane, *Phys. Rev. Lett.* **66**, 1529 (1991).
- ⁴² B. S. Shastry, *Phys. Rev. Lett.* **69**, 164 (1992).
- ⁴³ F. D. M. Haldane, Z. N. C. Ha, J. C. Talstra, D. Bernard, and V. Pasquier, *Phys. Rev. Lett.* **69**, 2021 (1992).
- ⁴⁴ N. Kawakami, *Phys. Rev. B* **46**, 1005 (1992).
- ⁴⁵ J. C. Talstra, Ph.D. thesis, Department of Physics, Princeton University, 1995.
- ⁴⁶ B. A. Bernevig, D. Giuliano, and R. B. Laughlin, *Phys. Rev. Lett.* **86**, 3392 (2001).
- ⁴⁷ M. Greiter and D. Schuricht, *Phys. Rev. Lett.* **96**, 059701 (2006).
- ⁴⁸ M. C. Gutzwiller, *Phys. Rev. Lett.* **10**, 159 (1963).
- ⁴⁹ T. A. Kaplan, P. Horsch, and P. Fulde, *Phys. Rev. Lett.* **49**, 889 (1982).
- ⁵⁰ W. Metzner and D. Vollhardt, *Phys. Rev. Lett.* **59**, 121 (1987).
- ⁵¹ Z. N. C. Ha and F. D. M. Haldane, *Phys. Rev. B* **47**, 12459 (1993).
- ⁵² J. C. Talstra and F. D. M. Haldane, *J. Phys. A: Math. Gen.* **28**, 2369 (1995).
- ⁵³ Z. N. C. Ha and F. D. M. Haldane, *Phys. Rev. Lett.* **73**, 2887 (1994), *ibid.* **74**, E3501 (1995).
- ⁵⁴ R. B. Laughlin, *Phys. Rev. Lett.* **50**, 1395 (1983).
- ⁵⁵ B. A. Bernevig, D. Giuliano, and R. B. Laughlin, *Phys. Rev. B* **64**, 024425 (2001).
- ⁵⁶ M. Greiter and D. Schuricht, *Phys. Rev. B* **71**, 224424 (2005).
- ⁵⁷ F. H. L. Eßler, *Phys. Rev. B* **51**, 13357 (1995).
- ⁵⁸ M. Hamermesh, *Group Theory and its Application to Physical Problems* (Addison-Wesley, Reading, Mass., 1962).
- ⁵⁹ T. Inui, Y. Tanabe, and Y. Onodera, *Group Theory and Its Applications in Physics* (Springer, Berlin, 1996).
- ⁶⁰ M. Greiter, *J. Low Temp. Phys.* **126**, 1029 (2002).
- ⁶¹ F. D. M. Haldane, *Phys. Lett.* **93 A**, 464 (1983).
- ⁶² F. D. M. Haldane, *Phys. Rev. Lett.* **50**, 1153 (1983).
- ⁶³ I. Affleck, in *Fields, strings and critical phenomena*, Vol. XLIX of *Les Houches lectures*, edited by E. Brézin and J. Zinn-Justin (Elsevier, Amsterdam, 1990).
- ⁶⁴ E. Fradkin, *Field Theories of Condensed Matter Systems*, No. 82 in *Frontiers in Physics* (Addison Wesley, Redwood City, 1991).
- ⁶⁵ I. Affleck, T. Kennedy, E. H. Lieb, and H. Tasaki, *Phys. Rev. Lett.* **59**, 799 (1987).
- ⁶⁶ I. Affleck, T. Kennedy, E. H. Lieb, and H. Tasaki, *Commun. Math. Phys.* **115**, 477 (1988).
- ⁶⁷ M. Greiter and S. Rachel, *Phys. Rev. B* **75**, 184441 (2007).
- ⁶⁸ M. Greiter, *Nat. Phys.* **6**, 5 (2010).
- ⁶⁹ F. Michaud, S. R. Manmana, and F. Mila, *Phys. Rev. B* **87**, 140404 (2013).
- ⁷⁰ J. Schwinger, in *Quantum Theory of Angular Momentum*, edited by L. Biedenharn and H. van Dam (Academic Press, New York, 1965).
- ⁷¹ A. Auerbach, *Interacting electrons and quantum magnetism* (Springer, New York, 1994).

⁷² G. Frobenius, *J. Reine Angew. Math.* **93**, 53 (1882).

⁷³ M. Greiter, X. G. Wen, and F. Wilczek, *Phys. Rev. Lett.*

66, 3205 (1991).

⁷⁴ C. Nayak and F. Wilczek, *Nucl. Phys. B* **479**, 529 (1996).